Lawrence Berkeley National Laboratory

Title
Assembly and Loading of LQS01, a Shell-Based 3.7 m Long Nb3Sn Quadrupole Magnet for LARP

Permalink
https://escholarship.org/uc/item/52d6d8b2

Author
Ferracin, P.

Publication Date
2010-06-01

Peer reviewed

Assembly and Loading of LQS01, a Shell-Based 3.7 m Long Nb₃Sn Quadrupole Magnet for LARP

P. Ferracin, G. Ambrosio, M. Anerella, B. Bingham, R. Bossert, S. Caspi, D. W. Cheng, G. Chlachidze, H. Felice, A. R. Hafalia, C. R. Hannaford, W. Mumper, F. Nobrega, S. Prestemon, G. L. Sabbi, J. Schmalzle, C. Sylvester, M. Tartaglia, P. Wanderer, and A. V. Zlobin

Accelerator Fusion Research Division
Ernest Orlando Lawrence Berkeley National Laboratory
University of California
Berkeley, California 94720

Assembly and Loading of LQS01, a Shell-Based 3.7 m Long Nb₃Sn Quadrupole Magnet for LARP

Assembly and Loading of LQS01, a Shell-Based 3.7 m Long Nb_3Sn Quadrupole Magnet for LARP

P. Ferracin, G. Ambrosio, M. Anerella, B. Bingham, R. Bossert, S. Caspi, D. W. Cheng, G. Chlachidze, H. Felice, A. R. Hafalia, C. R. Hannaford, W. Mumper, F. Nobrega, S. Prestemon, G. L. Sabbi, J. Schmalzle, C. Sylvester, M. Tartaglia, P. Wanderer, and A. V. Zlobin

Abstract—The LHC Accelerator Research Program (LARP) has been engaged in the fabrication of the 3.7 m long quadrupole magnet LQS01 in order to demonstrate that Nb_3Sn magnets are a viable option for future LHC Luminosity upgrades. The LQS01 design, a scale-up of the 1 m long Technology Quadrupole TQS, includes four 3.4 m long cos(theta) coils contained in a support structure based on four 1 m long aluminum shells pre-tensioned with water-pressurized bladders (shell-type structure). In order to verify assembly procedures and loading operations, the structure was pre-stressed around solid aluminum "dummy coils" and cooled-down to 77 K. Mechanical behavior and stress variations were monitored with strain gauges mounted on the structure and on the dummy coils. The dummy coils were then replaced with Nb_3Sn coils in a second assembly and loading procedure, in preparation for the cool-down and test. This paper reports on the cool-down test with dummy coils and on the assembly and loading of LQS01, with a comparison between 3D finite element model predictions and strain gauge data.

Index Terms—LARP, Nb_3Sn, quadrupole magnet.

I. INTRODUCTION

AFTER the tests of several 1 m long cos-theta type Technology Quadrupoles (TQ) [1]–[3] and of a 3.6 m Long Racetrack (LRS) magnet [4], [5], the LHC Accelerator Research Program (LARP [6], [7]) is now working on the test of the Long Quadrupole magnet LQS01, with the goal of demonstrating that Nb_3Sn is a mature technology for long accelerator-type superconducting magnets for future upgrades of the LHC Interaction Regions [8]. LQS01 features 3.4 m long cos-theta coils [9]–[11] contained in a support structure based on an external segmented aluminum shell pre-tensioned with water-pressurized bladders (shell-based structure). The design, procurement, and fabrication of the support structure were completed in 2008 at LBNL.
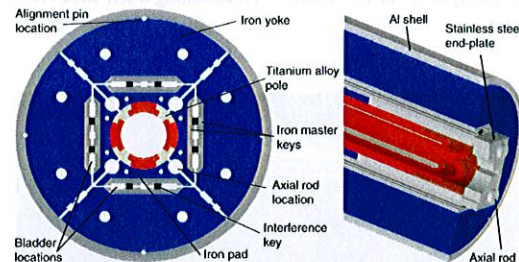
Fig. 1. LQS01 magnet cross-section (left) and end design (right).

To characterize its mechanical behavior and verify the finite element mechanical models, a 0.85 m long version of the structure was assembled around aluminum dummy coils, instrumented with strain gauges, and cooled-down to 77 K. The measured data, reported in [12], were consistent with finite element model predictions. In this paper, we provide an update on the LQS01 magnet development (see also [13]), focusing in particular on the assembly of the full-length structure, its mechanical qualification through a second cool-down test with aluminum dummy coils, and the final assembly and loading with the Nb_3Sn coils in preparation of the magnet test.

II. MAGNET DESIGN AND PARAMETERS

The LQS01 magnet design is shown in Fig. 1, while cable and magnet parameters are given in Table I. The structure features four yokes separated by open gaps and contained in an aluminum shell. Four pins at the magnet mid-planes provide alignment between the yoke quadrants and the shell. The coils are surrounded by four iron pads which, similarly to the yokes, include alignment slots for the insertion of iron master keys. The master keys provide alignment between pads and yokes. Additionally, they include grooves for the bladders, pressurized to pre-tension the shell and compress the coil, and for two interference keys, used to lock-in the pre-load. The coil ends are supported by two end plates connected with stainless steel rods. Shell and axial rod tensions are chosen so that the coils are still in contact with the titanium alloy poles, both in the straight section and in the ends, during excitation.

III. ASSEMBLY AND LOADING PROCEDURE

The assembly of the full length support structure started with the pre-assembly of four 0.85 m long segments, each of them composed by four yoke stacks inserted in an aluminum shell (Fig. 2). Before the insertion in the shell, the stacks were pre-compressed with a hydraulic cylinder and locked with 8

TABLE I
CABLE AND MAGNET PARAMETERS

Parameter	Unit	
Short sample current I_{ss} at 4.3 / 1.9 K	kA	13.88 / 15.31
Gradient at I_{ss} at 4.3 / 1.9 K	T/m	242 / 265
Coil peak field (layer 1) at I_{ss} at 4.3 / 1.9 K	T	12.39 / 13.56
Stored energy at I_{ss} at 4.3 / 1.9 K	kJ/m	473 / 570
Inductance	mH/m	4.9

Values computed based on extracted strand measurements
($J_c = 2720$ A/mm² at 4.2 K and 12 T), assuming a self-field correction of
0.483 T/kA.

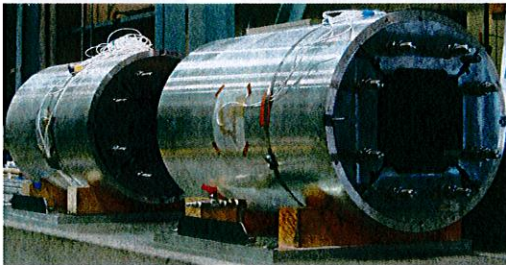Fig. 2. Two shell-yoke sub-assemblies before connection.

Fig. 3. Sequence of the connection of two shell-yoke sub-assemblies.

Fig. 4. LQSD dummy coil-pack and final assembly after pre-load.

stainless steel tie rods. The yoke-stacks are azimuthally aligned
through alignment pins set in grooves located in the yoke
laminations and in the shell inside diameter (Fig. 1).

The individual segments were then mounted on pneumatic
support systems and, after the removal of the 0.85 m tie rods,
maneuvered and connected to form two 1.7 m long sub-assem-
blies (Fig. 3) and, then, the full-length 3.4 m long shell-yoke
sub-assembly. The alignment pins, initially used to position
the yoke stacks inside the shell, were extended to guide the
connection operations and provide alignment between the
segments. 3.4 m long tie rods were used to draw and compress
the shell-yoke sub-assemblies. By means of a hydraulic system
the tie rods were pre-tensioned to 330 MPa, corresponding to
a total compressive force among the segments of 190 kN. This
high pre-load force was predetermined to guarantee, during all
magnet operations, full contact among the yoke laminations.
Under these conditions, the yoke stacks become the main
contributor to the flexural rigidity to whole structure. In parallel
to the assembly of the shell-yoke components, pad laminations
were stacked together and bolted around four 3.4 m long alu-
minum dummy coils (Fig. 4, left). The coil-pack sub-assembly
was then inserted into the shell-yoke sub-assembly, together
with master keys and bladders. The bladder pressurization was
then executed to push the yokes against the shell and compress
the coil-pack. Once the target shell tension was reached, inter-
ference keys were inserted in between the two master keys and
bladders were deflated and removed.

After the completion of the bladder operation, the coil axial
support system, composed by four, 25.4 mm diameter, stainless
steel axial rods with two stainless steel end-plates, 50 mm thick,
was installed. The axial rods, inserted in the clearance holes
between adjacent pads, were pre-tensioned to the target value
with a hydraulic piston, and the final axial force was locked-in
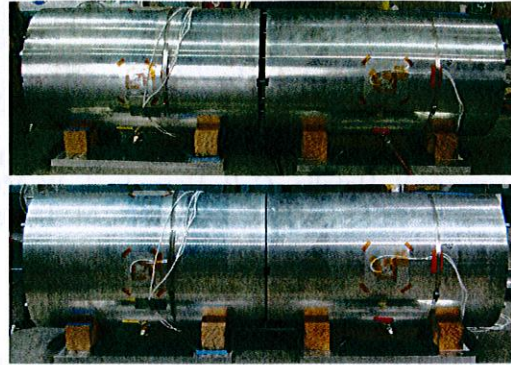with stainless steel nuts.

IV. COOL-DOWN TEST OF LQSD

The assembly and loading of the LQS structure around
dummy coils, called LQSD, were carried out at LBNL. LQSD
was then mounted on a dedicated fixture and shipped to FNAL
for a cool-down test to 77 K in a vertical cryostat.

A. LQSD Instrumentation

The LQSD mechanical behavior during cool-down was mon-
itored with strain gauges mounted on support structure compo-
nents and dummy coils. The shell was instrumented with half-
bridge strain gauges placed on each segment ("S1" to "S4" from
the lead end), and distributed on four mid-planes ("T" top, "R"
right, "B" bottom, and "L" left). The gauges measured both the
azimuthal ("T") and axial strain ("Z") and were all thermally
compensated by gauges mounted on stress-free aluminum ele-
ments. A similar configuration was adopted for the dummy coils
("D"), with gauges mounted along three axial positions ("1" to
$3''$ from the lead end) and on each of the four quadrants ("A" to
"D"), at the theoretical magnetic pole. Also, each axial rod was
equipped with two half-bridge gauges mounted close to the end
plate (lead end), in opposite azimuthal locations to compensate
for bending effects. In total, 36 gauges were mounted on LQSD.

B. LQSD Strain Gauge Data and 3D Model Results

The measurements of the LQSD azimuthal strain of the shell,
axial strain of the rods, and azimuthal strain of the dummy coils
are shown in Figs. 5to 7. The data, taken during cool-down from
293 K to 77 K, are compared with the predictions of a 3D finite
element model (described in [12]) of the entire magnet geom-
etry. The average values of the strain and stress measurements
($\pm 1\sigma$) are provided in Table II, together with the numerical ex-
pectations.

During cool-down, the measured shell azimuthal strain and
rod axial strain increased respectively from +535 to +1436 mi-
crostrain, and from +463 to +930 microstrain. Both measure-
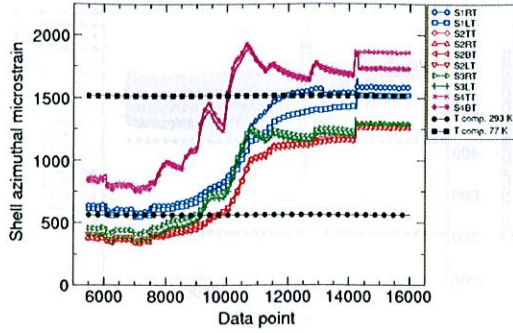ments were consistent with finite element model results. A close

Fig. 5. Measured and computed azimuthal (T) microstrain in the shell during LQSD cool-down.
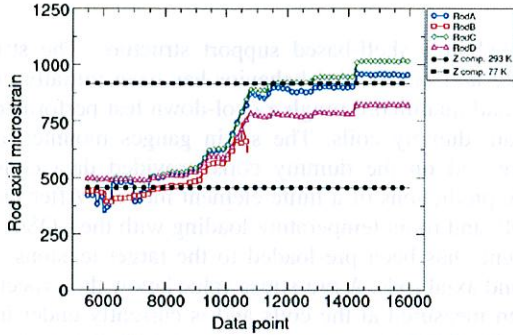

Fig. 6. Measured and computed axial (Z) strain in the rods during LQSD cool-down.
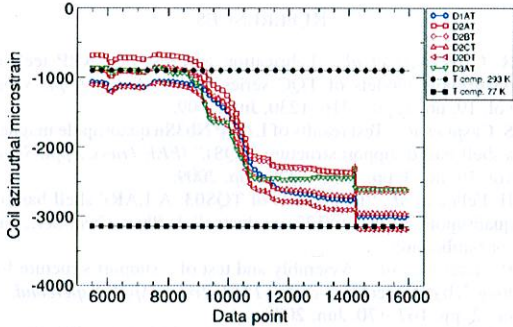

Fig. 7. Measured and computed azimuthal (T) strain in the dummy coils during LQSD cool-down.

look at the shell results in Fig. 5 points out that the azimuthal strain variations within individual shell segments are significantly smaller than the ±190 microstrain variation measured among the four segments. The spread between segments can be attributed to the shells' tolerances of fabrication, amounting to ±125 μm on the inner diameter. The large spikes observed in the segment S4, located at the bottom of the cryostat, resulted from sudden temperature reductions occurred when liquid nitrogen was poured into the cryostat.

The final tension in the aluminum shells determined an azimuthal compression of the dummy coil of −194 MPa, about 10% lower of the computed value, with a spread of ±25 MPa.

V. ASSEMBLY AND LOADING OF LQS01

Once the cool-down test was completed, LQSD was extracted from the vertical cryostat and shipped back to LBNL for un-

TABLE II
LQSD COMPUTED AND MEASURED (±1σ) STRAIN AND STRESS IN SHELL, DUMMY COILS, AND AXIAL RODS

293 K	ε_y (μstrain)	ε_z (μstrain)	σ_y (MPa)	σ_z (MPa)
Shell comp.	+563	−89	+42	+8
Shell meas.	+535 ±190	−165 ±111	+38 ±15	+1 ±10
Coil comp.	−897	+10	−71	−24
Coil meas.	−912 ±157	+106 ±90	−69 ±12	−16 ±7
Rod comp.	n/a	+455	n/a	+88
Rod meas.	n/a	+463 ± 38	n/a	+89 ± 7
77 K	ε_y (μstrain)	ε_z (μstrain)	σ_y (MPa)	σ_z (MPa)
Shell comp.	+1517	−56	+133	+41
Shell meas.	+1436 ±222	+16 ±183	+127 ±18	+44 ±14
Coil comp.	−3147	+1837	−225	+66
Coil meas.	−2835 ±248	+1870 ±231	−194 ±25	+80 ±24
Rod comp.	n/a	+917	n/a	+191
Rod meas.	n/a	+930 ±99	n/a	+195 ±21

loading and disassembly. The iron pads were then bolted around the LSQ01 coils (coil #6 to #9), which were wound at FNAL and reacted and impregnated at BNL and FNAL. The coils were instrumented with strain gauges mounted on the titanium-alloy winding poles. The coil-pack was then inserted in the shell-yoke sub-assembly and pre-loaded with a bladder operation, replicating the same procedures as LQSD's.

A. LQS01 Instrumentation

Each of the four LQS01 coils' ("C") poles were instrumented on the inner layer with azimuthal ("T") and axial ("Z") gauges mounted along four axial locations ("1" to "4" from the lead end), and, again, they were thermally compensated. The total number of gauges mounted on the LQS01 magnet amounts to 56 gauges.

B. LQS01 Strain Gauge Data and 3D Model Results

The strain in shell segments, rods, and coil winding poles was monitored during all LQS01 room temperature pre-loading operations, and the results are plotted in Figs. 9to 11, together with the numerical expectations. The average values of the strain and stress measurements (±1σ) are given in Table III. The shell and the axial rods were pre-loaded respectively to +33 MPa of azimuthal stress and +60 MPa of axial stress, corresponding, according the finite element model, to the room temperature pre-load values for a gradient of 230-240 T/m. The shell variations in azimuthal tension decreased from ±15 MPa, measured in LQSD, to ±8 MPa. The spikes seen in Fig. 9 are the results of the bladder pressurization stages, which allowed the insertion of shims with increasing thickness until the average shell tension reached the target value of about 450 microstrain.

Fig. 11 shows the data relative to the coil winding poles: the "zero strain condition" was set as the status of the coils after the bolting of the pads, before the insertion of the coil-pack inside the shell-yoke sub-assembly (Fig. 8). The final azimuthal stress of −12 MPa is lower than the expected −49 MPa. At the moment, the causes of this inconsistency between measured and computed values are not clear. Since it was not observed in the LQSD room temperature data, it is possible that such a difference may be related to initial discrepancies or non-uniformities in coil radial and azimuthal dimensions with respect to the nominal ones. It is expected that the strain gauge data taken after

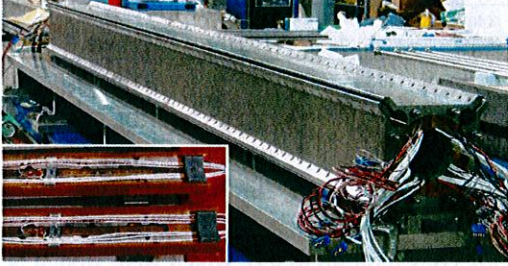| 293 K	ε_y (μstrain)	ε_z (μstrain)	σ_y (MPa)	σ_z (MPa)
Shell comp.	+447	-71	+34	+6
Shell meas.	+451 ±113	-113 ±108	+33 ±8	+3 ±7
Pole comp.	-344	+9	-49	-14
Pole meas.	-125 ±71	+135 ±119	-12 ±11	+14 ±17
Rod comp.	n/a	+327	n/a	+63
Rod meas.	n/a	+310 ±18	n/a	+60 ±3

Fig. 8. LQS01 coil-pack sub-assembly, with a close-up of the two coils (return end) at the end of the instrumentation process.
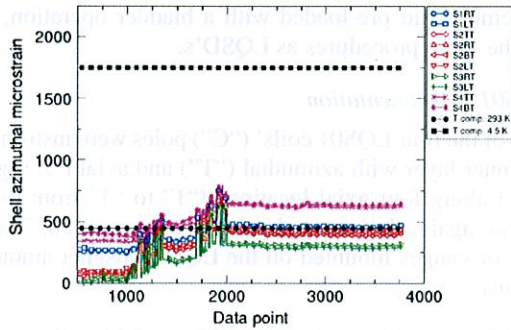

Fig. 9. Measured and computed azimuthal (T) strain in the shell segments during LQS01 room temperature pre-load.
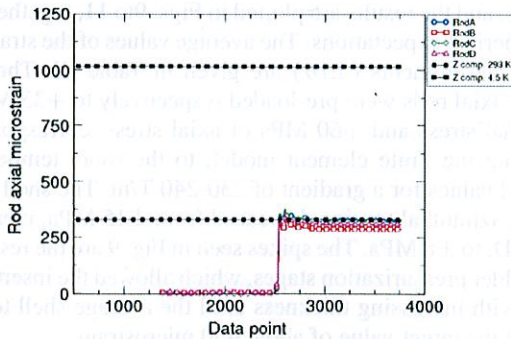

Fig. 10. Measured and computed axial strain (Z) in the rods during LQS01 room temperature pre-load.

cool-down and during excitation will provide a clearer picture of the coil pre-stress level, as shown in [3].

VI. CONCLUSION

The magnet LQS01, a LARP Nb₃Sn quadrupole implementing 3.4 m long cos-theta coils, has been assembled and
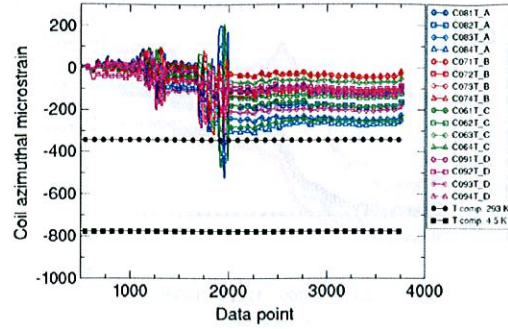

Fig. 11. Measured and computed azimuthal (T) strain in the coil winding poles during LQS01 room temperature pre-load.

pre-loaded in a shell-based support structure. The structure assembly and mechanical behavior has been initially characterized and qualified through a cool-down test performed with aluminum dummy coils. The strain gauges mounted on the structure and on the dummy coils provided data consistent with the predictions of a finite element models. After the final assembly and room temperature loading with the LQS01 coils, the magnet has been pre-loaded to the target tensions on the shells and axial rods. A pre-stress value below the expectations has been measured at the coils and is currently under investigation. The LQS01 quadrupole is now ready for its first test, which will be executed at FNAL by the end of 2009.

REFERENCES

[1] R. C. Bossert et al., "Fabrication and test of LARP technological quadrupole models of TQC series," IEEE Trans. Appl. Supercond., vol. 19, no. 3, pp. 1216–1230, Jun. 2009.

[2] S. Caspi et al., "Test results of LARP Nb3Sn quadrupole magnets using a shell-based support structure (TQS)," IEEE Trans. Appl. Supercond., vol. 19, no. 3, pp. 1221–1225, Jun. 2009.

[3] H. Felice et al., "Test results of TQS03: A LARP shell-based Nb3Sn quadrupole using 108/127 conductor," J. Phys. Conf. Ser., submitted for publication.

[4] P. Ferracin et al., "Assembly and test of a support structure for 3.6 m long Nb3Sn racetrack coils," IEEE Trans. Appl. Supercond., vol. 18, no. 2, pp. 167–170, Jun. 2008.

[5] J. F. Muratore et al., "Test results of LARP 3.6 m Nb3Sn racetrack coils supported by full-length and segmented shell structures," IEEE Trans. Appl. Supercond., vol. 19, no. 3, pp. 1212–1216, Jun. 2009.

[6] P. Wanderer, "Overview for LARP magnet R&D," IEEE Trans. Appl. Supercond., vol. 19, no. 3, pp. 1208–1211, Jun. 2009.

[7] P. Ferracin, "LARP Nb3Sn quadrupole magnets for the LHC luminosity upgrade," in AIP Conf. Proc., to be published.

[8] V. Baglin, Conceptual Design of the LHC Interaction Region Upgrade—Phase-I LHC Project Report 1163, 2008, et al..

[9] G. Ambrosio et al., "LARP long Nb3Sn quadrupole design," IEEE Trans. Appl. Supercond., vol. 18, no. 2, pp. 268–272, Jun. 2008, also in LBNL Report 1033E, June 2008.36.

[10] G. Ambrosio et al., "Development and coil fabrication for the LARP 3.7-m long Nb3Sn quadrupole," IEEE Trans. Appl. Supercond., vol. 19, no. 3, pp. 1231–1234, Jun. 2009.

[11] H. Felice et al., "Instrumentation and quench protection for LARP Nb3Sn magnets," IEEE Trans. Appl. Supercond., vol. 19, no. 3, pp. 2458–2462.38, Jun. 2009.

[12] P. Ferracin et al., "Fabrication and test of a 3.7 m long support structure for the LARP Nb3Sn quadrupole magnet LQS01," IEEE Trans. Appl. Supercond., vol. 19, no. 3, pp. 1106–1111, Jun. 2009.

[13] G. Ambrosio et al., "Final development and test preparation of the first 3.7 m long Nb3Sn quadrupole by LARP," IEEE Trans. Appl. Supercond., submitted for publication.